Int. J. Plant Sci. 182(7):649–662. 2021.

1058-5893/2021/18207-0006$15.00 DOI: 10.1086/715506

GEOCHEMICAL FINGERPRINTS OF GINKGOALES ACROSS THE TRIASSIC-JURASSIC BOUNDARY OF GREENLAND

Vivi Vajda,[1,*] Milda Pucetaite,[1,†] and Margret Steinthorsdottir*,‡

*Department of Palaeobiology, Swedish Museum of Natural History, SE-104 05 Stockholm, Sweden; †Centre for Environmental and Climate Science, Lund University, SE-223 62 Lund, Sweden; and ‡Bolin Centre for Climate Research, Stockholm University, SE-109 61 Stockholm, Sweden

Guest Editor: Anne-Laure Decombeix

Premise of research. Geochemical fingerprinting of fossil plants is a relatively new research field complementing morphological analyses and providing information for paleoenvironmental interpretations. Ginkgoales contains a single extant species but was diverse through the Mesozoic and is an excellent target for biochemical analyses.

Methodology. Cuticles derived from fresh and fallen autumn leaves of extant *Ginkgo biloba* and seven fossil ginkgoalean leaf taxa, one seed fern taxon, and two taxa with bennettitalean affinity were analyzed by infrared (IR) microspectroscopy at the D7 beamline in the MAX IV synchrotron laboratory, Sweden. The fossil material derives from Triassic and Jurassic successions of Greenland. Spectral data sets were compared and evaluated by hierarchical cluster analysis (HCA) and principal component analysis performed on vector-normalized, first-derivative IR absorption spectra.

Pivotal results. The IR absorption spectra of the fossil leaves all reveal signatures that clearly indicate the presence of organic compounds. Spectra of the extant *G. biloba* leaves reveal the presence of aliphatic chains, aromatic and ester carbonyl functional groups from polymer cutin and other waxy compounds, and polysaccharides. Interestingly, both the extant autumn leaves and the fossil specimens reveal the presence of carboxyl/ketone molecules, suggesting that chemical alterations during the initial stages of decomposition are preserved through fossilization. Two major subclusters were identified through HCA of the fossil spectra.

Conclusions. Consistent chemical IR signatures, specific for each fossil taxon are present in cuticles, and sufficient molecular content is preserved in key regions to reflect the plants' original chemical signatures. The alterations of the organic compounds are initiated as soon as the leaves are shed, with loss of proteins and increased ester and carboxyl/ketone compound production in the fallen leaves. We further show that the groupings of taxa reflect a combination of phylogeny and environmental conditions related to the end-Triassic event.

Keywords: paleobotany, *Ginkgo*, chemotaxonomy, proteins, CO_2, climate.

Online enhancements: supplementary table and figure.

Introduction

Fossil plant phylogenies are typically based on morphological characters, especially those of the reproductive structures. However, these are unavailable for many taxa, and in many cases, only fragmentary foliage is available for study. In addition to morphological characters, studies of remnant organic constituents within fossils have shown to be important for supporting taxonomic and phylogenetic assignations (D'Angelo 2010, 2015; Vajda et al. 2017) and even reconstructing overall architecture of fragmented fronds (D'Angelo et al. 2018; Zodrow et al. 2019). Infrared (IR) microspectroscopy has proven to be a particularly useful technique for this purpose because of its nondestructive nature, chemical specificity, and ability to analyze minute sample areas, which enables analysis of, for instance, fossil pollen and spores (e.g., Steemans et al. 2010; Fraser et al. 2012; Jardine et al. 2016, 2019; Dupont-Nivet 2021), minute leaf fragments (Vajda et al. 2017), fossil resin (Seyfullah et al. 2015), and even fossilized cellular organelles (Qu et al. 2019). IR microspectroscopy has been employed for the identification of organic compounds in various fossils, such as pre-Cambrian stromatolites and fungi (Qu et al. 2015), but also for advanced multicellular organisms. For example, this technique has demonstrated the presence of original organic compounds in the skin and bones of Mesozoic dinosaurs (Boatman et al. 2019) and marine reptiles (Lindgren et al. 2014, 2018).

Fossil leaf cuticles are widely used in paleobotany because of their high preservation potential (van Bergen et al. 1978; Barclay et al. 2007; Guignard et al. 2019). As early as the 1920s, Harris (1926) stated that "the composition of the cuticle seems to vary and be of some phylogenetic importance." Through acid maceration of fossil leaves, he noticed that fossil fern cuticles dissolved more readily when treated with HNO_3 followed by $KClO_3$, whereas seed plant cuticles withstood the maceration process.

[1] Authors for correspondence; email: vivi.vajda@nrm.se, milda.pucetaite@cec.lu.se. These authors contributed equally to this work.

Manuscript received December 2020; revised manuscript received May 2021; electronically published July 15, 2021.

When analyzing the organic compounds of fossil cuticles, however, an important aspect to consider is their diagenetic history (D'Angelo et al. 2011; D'Angelo and Zodrow 2020). On the other hand, given similar preservation states, chemical differences between the fossil cuticles of various plants may reflect original compositional differences of the cuticle and even aid in resolving taxonomic relationships between plant groups (D'Angelo and Zodrow 2015). Furthermore, IR microspectroscopy has been applied to assess cuticular chemical variations in extant plants upon exposure to environmental triggers, such as increased levels of UV at high altitudes (Lomax et al. 2012), heat stress (Liu et al. 2019), and contrasting levels of atmospheric carbon dioxide concentration (pCO_2) under changing climates (Jardine et al. 2019). Fraser et al. (2011) conducted a study on the relationship between the UVB regime and aromatic pigment content in modern pollen and could show that birch pollen biochemically adapt to their local UV environment. In another interesting study, Jardine et al. (2020) reconstructed surface UVB irradiance over a time span of the past 650 yr by means of a UVB proxy based on the chemical signature of *Pinus* pollen. They could substantiate a positive relationship between the abundance of UVB-absorbing compounds in the pollen and modeled solar UVB irradiance.

Given that the environment-specific chemical composition is reflected in the organic molecules preserved in pollen grains and cuticles, IR spectroscopic analyses of fossils can provide crucial information about climates of the past, as demonstrated via analysis of pollen (Jardine 2016, 2017, 2020; Dupont-Nivet 2021). Such environmental signals in the plant tissue might complicate the use of IR microspectroscopy for accurate taxonomic or phylogenetic analysis but in turn add another available proxy.

The gymnosperm order Ginkgoales contains a single living species (*Ginkgo biloba*), yet it is represented by a diverse range of fossil leaf taxa through the entire Mesozoic, generally with well-preserved cuticles. Ginkgoales is most commonly regarded as the sister group to Coniferales (Pinales) and Cordaitales (Florin 1949; Taylor et al. 2009; McLoughlin 2017, 2021), but there is also evidence favoring a closer relationship with seed ferns, such as Peltaspermales (Meyen 1984; Anderson and Anderson 2003) and Umkomasiales (corystosperms; Gordenko and Broushkin 2015 and references therein). Ginkgoales originated in the Paleozoic and was a major and diverse component of the global flora throughout the Mesozoic (Taylor and Taylor 1993; Royer et al. 2003; Zhou 2009; Bauer et al. 2013; Kustatscher et al. 2018; McLoughlin 2021). The oldest record of *Ginkgo* is from the Triassic, making it the oldest extant seed plant genus (Zhou and Wu 2006). The abundance and diversity of the most common morphogenera *Ginkgoites*, *Baiera*, and *Sphaenobaiera* increased dramatically from the Late Triassic into the Jurassic and Early Cretaceous, after which the Ginkgoales declined (Taylor and Taylor 1993; Royer et al. 2003; Zhou and Wu 2006; McElwain et al. 2007; Crane 2019). The few *Ginkgo* species identified from Cenozoic strata are very similar to the only extant species, and it is possible that these are in fact conspecific with *G. biloba* (Tralau 1968; Mustoe 2002; Royer et al. 2003).

Molecular analyses of *Ginkgo* plants from China have shown over the past two decades that genetic diversity is higher among *Ginkgo* populations than previously considered and that two separated refugia existed following the Pleistocene glaciations in China (Ge et al. 2003; Fan et al. 2004; Shen et al. 2005; Gong et al. 2008). Today, *G. biloba* is all but extinct in the wild, probably forced by the Pleistocene glaciations combined with increased competition from angiosperms, and it propagates naturally in the wild only in restricted geographic areas in eastern and central China (Gong et al. 2008; Crane 2019). Although *G. biloba* thrives best in temperate and mesic climates, just like its Mesozoic ancestors, it has become a very popular ornamental plant in parks and along city streets and is planted and cultivated all over the world in many climate zones.

Extant and fossil members of Ginkgoales and the sister group, Czekanowskiales (Leptostrobales), have dimorphic shoots, with leaves attached to long and short shoots (Harris 1937; Lundblad 1959*a*, 1959*b*; Taylor et al. 2006). *Ginkgo biloba* is dioecious, with male plants preferentially grown in cities, and the plant yields one of the most popular herbal medicines, generally derived from leaf extracts, which purportedly has positive effects on neurodegenerative and cardiovascular diseases (Zhou et al. 2019). Standardized *G. biloba* extract (EGb 761) from leaves typically contains "24% flavonoid glycosides, 6% terpene lactones and less than 5 ppm ginkgolic acid" (Smith and Luo 2004, p. 446).

Leaves of *Ginkgo* and other ginkgoaleans bear the vast majority of their stomata on the thinner abaxial (lower) epidermis (hypostomatous; e.g., Beerling et al. 1998; Chen and Li 2004). Stomatal densities of plant leaves have an empirically and experimentally demonstrated inverse relationship with atmospheric pCO_2, and this relationship can be applied to reconstruct pCO_2 from the past using fossil leaves (Woodward 1987; Richard et al. 2007). Gingkoalean leaves are arguably the most important and common fossils for pCO_2 reconstruction and to infer past climates because of the group's relatively consistent leaf morphology through time and its long and abundant fossil record (Beerling et al. 1998; McElwain et al. 1999; Chen et al. 2001; Retallack 2001; Royer et al. 2003; Sun et al. 2007; Quan et al. 2009; Smith et al. 2010; Barbacka 2011; Steinthorsdottir et al. 2011*b*; Mays et al. 2015; Meller et al. 2015; Barclay and Wing 2016; Sun et al. 2016, 2018; Wu et al. 2016; Zhang et al. 2019; Retallack and Conde 2020; Zhou et al. 2020).

The Triassic-Jurassic Paleoenvironment

The Triassic and Jurassic periods were typical greenhouse intervals characterized by warm climates and high pCO_2 resulting in an absence of polar ice caps and highly diverse ecosystems with lush mid- and high-latitude vegetation (e.g., McElwain et al. 2007, 2009; Jansson et al. 2008; Kustatscher et al. 2018). The studied specimens grew in moist environments, such as waterlogged floodplains, riverbanks, and swamps, and ginkgoaleans were an important, but far from dominant, component of the vegetation (Harris 1937; Lundblad 1949; McElwain et al. 2007; Vajda and Wigforss-Lange 2009). The end of the Triassic was marked by a mass extinction (Sepkoski 1996) with a major vegetation turnover (Harris 1937; McElwain et al. 2007; Pott and McLoughlin 2011; Vajda et al. 2013; Lindström et al. 2017; Kustatscher et al. 2018). The prevailing consensus is that massive volcanic activity in the Central Atlantic Magmatic Province, linked to the opening of the Atlantic Ocean, was the primary trigger for the extinctions via the release over a relatively short time interval of vast amounts of greenhouse gases, including CO_2, causing abrupt global warming of ~3°–4°C (Yapp and Poths 1996; McElwain et al. 1999; Lindström et al. 2017). Stomatal densities reveal that pCO_2 at least doubled, increasing from ~1000 ppm in the Late

Triassic to 2000–2500 ppm at the Triassic-Jurassic boundary and in the earliest Jurassic (fig. 1; McElwain et al. 1999; Bonis et al. 2010; Barbacka 2011; Steinthorsdottir et al. 2011*b*; Mander et al. 2013; Steinthorsdottir and Vajda 2015; Wu et al. 2016; Slodownik et al. 2021). This was accompanied by disruptions to the hydrological (Steinthorsdottir et al. 2012) and carbon cycles, supported by $\delta^{13}C$ records (Olsen 1999; Hesselbo et al. 2002; Akikuni et al. 2010; Bacon et al. 2011; Pálfy and Kocsis 2014; Marzoli et al. 2018; Schobben et al. 2019; Kovács et al. 2020). The earliest Jurassic saw extremely elevated pCO_2 (>2000 ppm), and locally, the hydrological cycle was disrupted because of the suppression of plant transpiration, leading to increased surface water availability and a more open landscape (Steinthorsdottir et al. 2011*b*, 2012). Following the end-Triassic floral turnover, Ginkgoales became a dominant component of the vegetation in high-latitude Northern Hemisphere ecosystems, whereas other taxa that had previously dominated, such as the bennettites *Anomozamites* and *Pterophyllum*, became minor components (e.g., McElwain et al. 2007; Steinthorsdottir et al. 2011*a*; Barbacka et al. 2014; Soh et al. 2017; Kustatscher et al. 2018).

Here, we use IR microspectroscopy to analyze fossil gingkoalean cuticles from the Astartekløft succession of eastern Greenland spanning the Triassic-Jurassic boundary (figs. 1–3) and modern *G. biloba* leaves, both fresh leaves and fallen autumn leaves. Additionally, we analyzed peltaspermalean and bennettitealean leaves from the same succession at Astartekløft to test them as an out-group. The aims of this study are to assess whether the IR absorption spectra of the fresh and fallen *G. biloba* leaves are differentiable and how they compare with the spectra of the fossil leaves; whether the biochemical signatures of the fossil leaves demarcate distinct groupings within the order, aiding systematic placement of the ginkgoalean taxa; and whether environmental

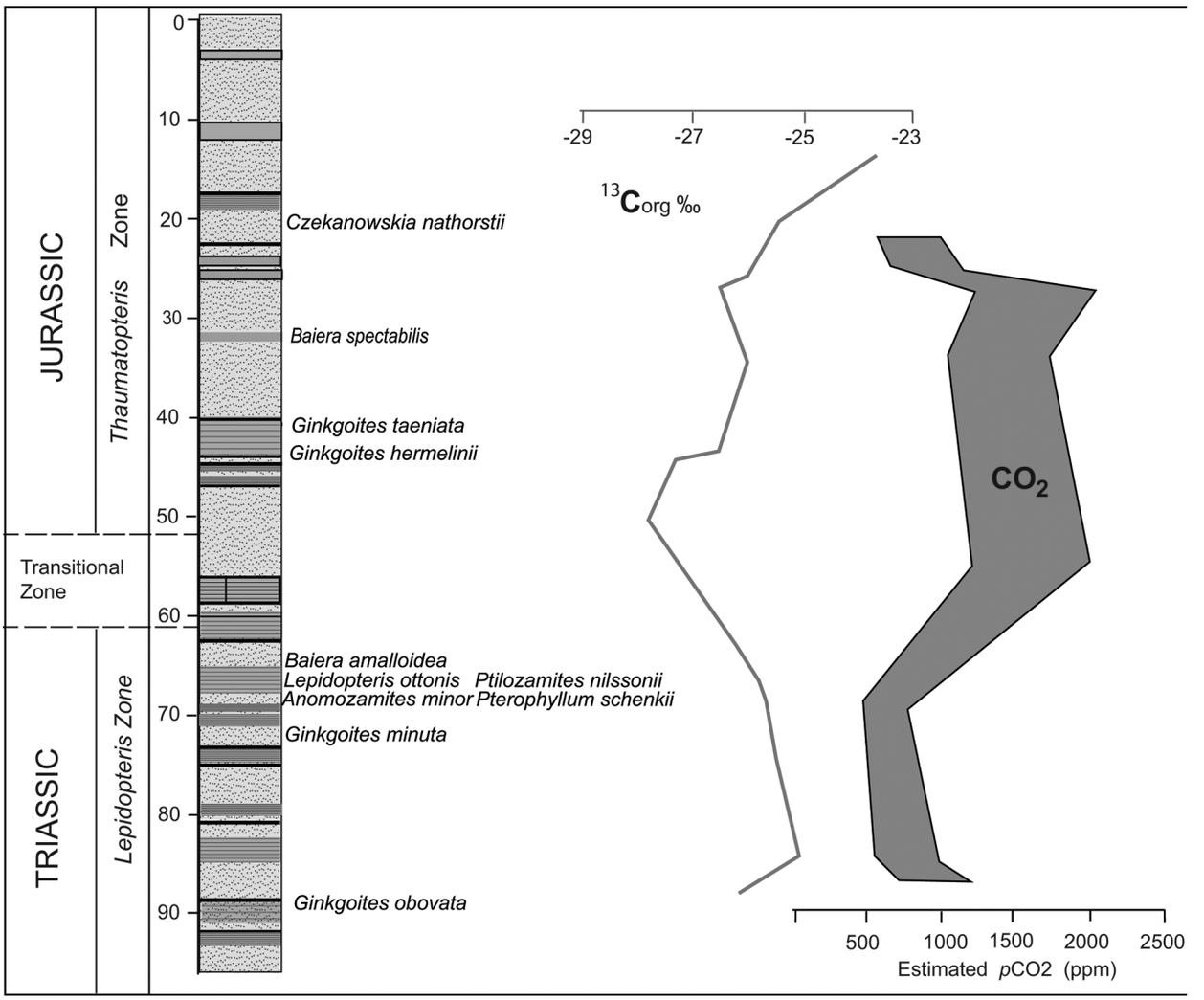

Fig. 1 Fossil specimens analyzed by infrared microspectroscopy in this study, organized stratigraphically across the section at Astartekløft spanning the Triassic (Rhaetian)–Jurassic (Hettangian) boundary, modified after McElwain et al. (2007). Plotted against the log: organic carbon isotopic signal from cuticles and a paleoatmospheric CO_2 record based on cuticles from McElwain et al. (1999). A color version of this figure is available online.

conditions, such as temperature or atmospheric pCO_2, may have influenced the geochemical fingerprints of the fossil leaves.

Material and Methods

The fossil leaves studied herein derive from the sedimentary succession at Scoresby Sound, East Greenland (fig. 1), deposited during the Triassic-Jurassic transition (fig. 1). IR absorption spectra of cuticles from the seven fossil *Ginkgoites* leaf species—*Ginkgoites obovata* Nathorst (Seward), *Ginkgoites minuta* Nathorst (Lundblad), *Ginkgoites hermelinii* Nathorst (Hartz), and *Ginkgoites taeniata* (Geinitz) Frenguelli and the related sister taxa *Baeira amalloidea* Harris, *Baeira spectabilis* Nathorst, and *Czekanowskia nathorstii* Harris—were compared with each other and with the only extant *Ginkgo* species—*Ginkgo biloba* (figs. 1–5). For additional comparisons, cuticles of nonginkgophyte seed plants from the same succession were analyzed, including *Lepidopteris ottonis* (Göppert) Schimper, *Pterophyllum schenkii* Zeiller, *Ptilozamites nilssonii* Nathorst, and *Anomozamites minor* (Brongniart) Nathorst emend. Pott et McLoughlin.

The fossil leaves were collected by Thomas Harris in 1926 and 1927 as part of the Danish state expeditions to East Greenland, and the macroplants collected during these expeditions are described in the iconic volumes on the Scoresby Sound flora (Harris 1931, 1932*a*, 1932*b*, 1935, 1937). The paleobotanical collection is held in the Natural History Museum of Denmark, Copenhagen. For consistency, we have followed the original taxonomy, spelling, and ID numbering of specimens outlined by Harris (1932*a*, 1932*b*, 1935, 1937). We consistently used fossil cuticle free from any mesophyll or coal for our analyses, as previous results have shown that different functional groups may be present depending on whether the leaf fossils are represented by cuticle alone (typified by highly aliphatic compounds) or whether the compressions incorporate portions of coalified mesophyll (D'Angelo et al. 2011). Cuticle was carefully peeled from the rock and analyzed without any further treatment. There is one exception, however, and that is *A. minor*, which was treated with HCl and HF followed by HNO_3 and $KClO_3$. Importantly, the lithologies of the plant-bearing beds sensu Harris (1931) hosting the fossils of "large and even undamaged leaves" are similar through the Scoresby Sound succession and are represented by laminated mudstones set between otherwise thick packages of cross-bedded sandstones barren of fossils (Harris 1937).

The cuticles of extant *G. biloba* derive from the leaves of an old, large *G. biloba* tree growing in the Lund botanical gardens, Lund, Sweden. The tree, which is the oldest *Ginkgo* in Sweden, was brought as a seedling from China around 1870 by Jacob Georg Agardh, professor of botany in 1853–1879. In addition to fresh leaves from the tree, we collected fallen yellow autumn leaves to assess chemical changes within the cuticles during the initial stages of desiccation and decomposition. Cuticle of the

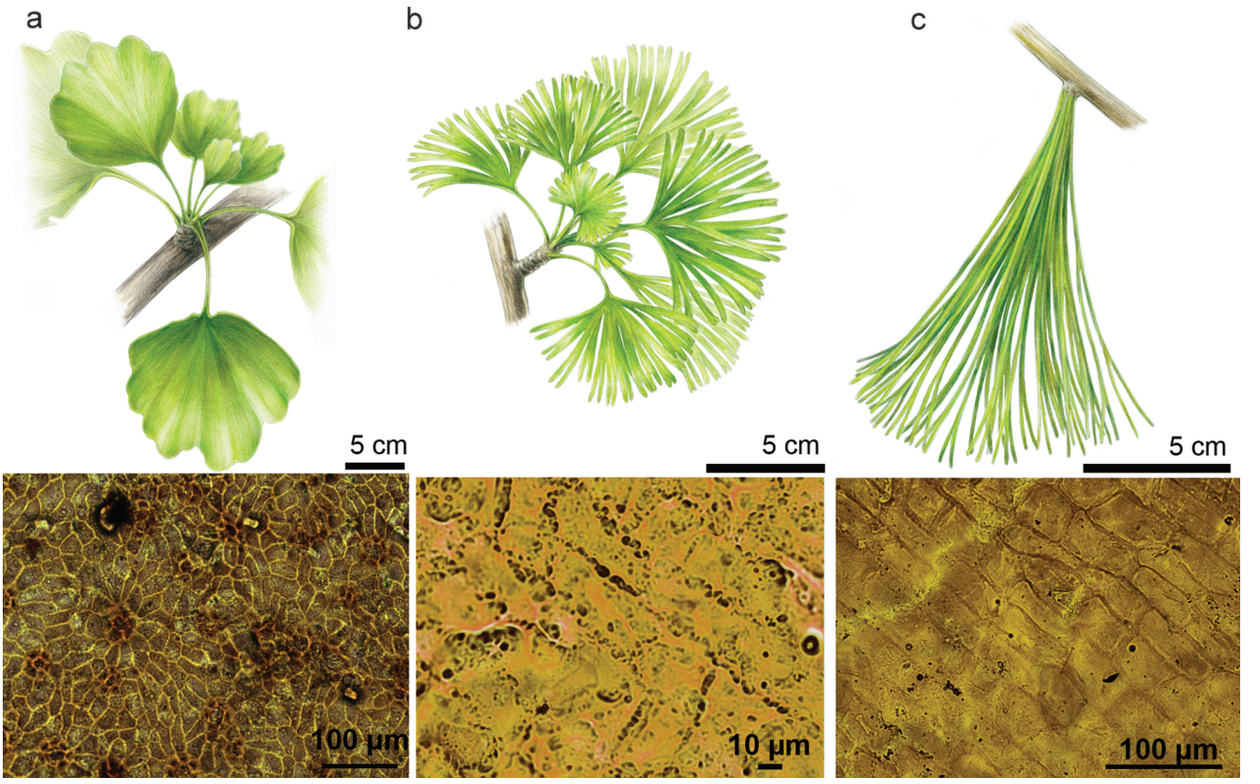

Fig. 2 Illustrated reconstructions of selected ginkgoalean taxa with corresponding micrograph of leaf cuticles; these are not the analyzed fragments but representative specimens from Harris (1935). *a*, *Ginkgoites obovata*, ID 2420. *b*, *Ginkgoites minuta*, ID 2495. *c*, *Czekanowskia nathorstii*, ID 2967. Illustrations are based on photographs of Harris's original specimens.

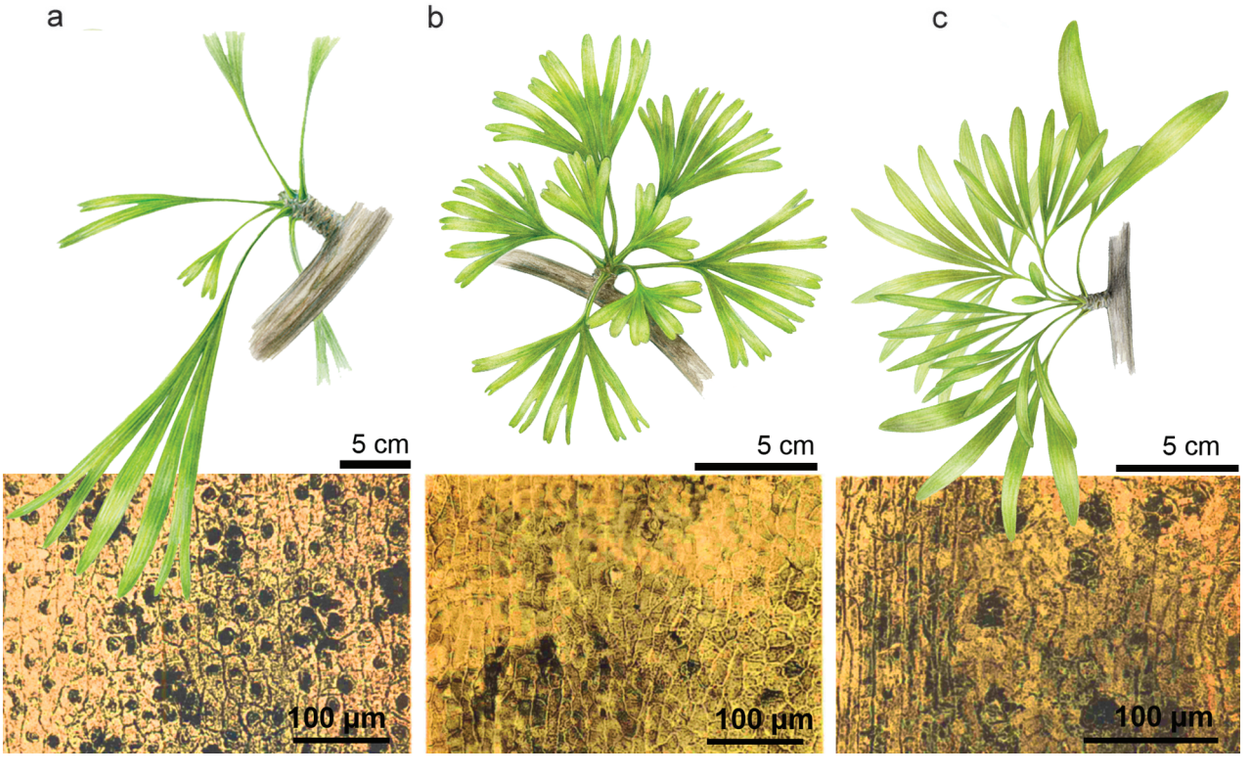

Fig. 3 Illustrated reconstructions of selected ginkgoalean taxa with corresponding micrograph of leaf cuticles; these are not the analyzed fragments but representative specimens from Harris (1935). *a*, *Baeira spectabilis*, ID 2675. *b*, *Ginkgoites taeniata*, ID 2352. *c*, *Ginkgoites hermelinii*, ID 2554. Illustrations are based on photographs of Harris's original specimens.

extant *G. biloba* was peeled directly from the surface of the fresh leaf with no chemical processing and was then dried in a vacuum chamber. Subsequently, IR microspectroscopic analysis was carried out.

The reconstructions in figures 2 and 3 are original illustrations, never previously published, and prepared by the department's illustrator, Pollyanna von Knorring, under the instruction of the authors. We used fossil specimens from the collections combined with line drawings by Nathorst, Harris, and Lundblad to produce the most accurate reconstruction.

Experimental methods. The experimental and data analysis procedure was outlined by Vajda et al. (2017). Briefly, IR microspectroscopy measurements were performed at the currently decommissioned D7 beamline at the MAX IV synchrotron facility, Lund University, Lund, Sweden. A Hyperion 3000 IR microscope combined with a Fourier transform IR spectrometer IFS 66v/S (Bruker Optik, Ettlingen, Germany) with globar light source and KBr beam splitter was used for the measurements. The microscope is equipped with a single-element liquid-nitrogen-cooled mercury cadmium telluride detector. A ×15/0.4 objective was used. A knife-edge aperture that limits the size of the beam on the sample was adjusted according to the size of the cuticles when collecting the spectra to prevent stray light (radiation that propagates through areas without sample) from reaching the detector. Spectra in the range of 4000–850 cm^{-1} were recorded using a spectral resolution of 4 cm^{-1}. The lower wave number limit is determined by the use of the CaF_2 optical window as a sample substrate. We averaged 128 interferograms, and the result was Fourier transformed into a spectrum applying the Blackmann-Harris 3 apodization function and zero-filling factor 2. At least three separate cuticles of each taxon were analyzed, and several spectra were recorded in multiple locations on each cuticle sample. Algorithms of atmospheric compensation and baseline correction (rubber band method) were applied to three selected spectra of high quality (no saturated absorptions, high signal-to-noise ratio, no significant baseline oscillations due to scattering) in accordance with spectral preprocessing as previously described (Baker et al. 2014). The algorithms are default functions of the OPUS software (Bruker Optik, Ettlingen, Germany). Subsequently, the spectra were analyzed using a script written in the MATLAB package (ver. 7.14; MathWorks), as it allows for better control of the processing.

Data analysis. Spectral data sets obtained by IR microspectroscopy were evaluated by multivariate approaches—hierarchical cluster analysis (HCA) and principal component analysis (PCA)—performed on vector-normalized, first-derivative (calculated by the Savitzky-Golay algorithm using a polynomial of degree two and window size of nine points) spectra (Ami et al. 2013; Gautam et al. 2015). We have experimentally found that these preprocessing parameters best emphasize overlapping spectral features without significant loss in signal-to-noise ratio (Mark and Workman 2003). The fingerprint spectral region within limits of 1850–1300 cm^{-1} was selected and used for both HCA and PCA. It contains the most information on the molecular content

of the samples (Domenighini and Giordano 2009). In addition, in our previous work we tested the effects of using expanded and different spectral ranges and found that the fingerprint region yields the most stabile results (Vajda et al. 2017). The region below 1300 cm^{-1} was excluded to avoid the influence of kaolinite spectral bands (e.g., at 1115, 1034, 1008, and 913 cm^{-1} with shoulder at 939 cm^{-1}) on the analysis results (Cruz and Duro 1999). We chose to use all data points within the selected spectral range in the analysis instead of individual bands in order to include all possibly important spectral signatures. For the HCA, Euclidean distances between the spectra were calculated, then Ward's algorithm was used to group the data. The fingerprint region contains the most information on the molecular content of the samples (Domenighini and Giordano 2009). The hierarchical clustering results were displayed in the form of dendrograms in which the heterogeneity factor—Euclidean distance—represents proximity between the clusters. An algorithm of optimal leaf ordering (Bar-Joseph et al. 2001) was applied for the adjacent clusters to have the highest similarity.

A heat map was plotted using the clustergram function (MATLAB) with no clustering applied on the wave numbers. PCA was performed using the PCA function (MATLAB).

Code availability. The data and MATLAB code used for HCA and PCA are available on GitHub (https://github.com/mildapu/fossil-cuticle-spectral-analysis).

Results and Interpretation

Spectral Results

In accordance with previous studies (Vajda et al. 2017), IR absorption spectra of the modern *Ginkgo biloba* cuticles (figs. 4, 5*a*) contain characteristic spectral bands of lipidic polyester cutin and waxes corresponding to CH_2, CH_3 stretching and bending vibrations of long aliphatic chains (at 2958, 2919, 2872, 2850, 1469, 1442, 1414, and 1373 cm^{-1}), and C=O stretching vibrations of ester carbonyl (at 1734 cm^{-1}). Broad spectral features in the wave number region between 1700 and 1480 cm^{-1} are due

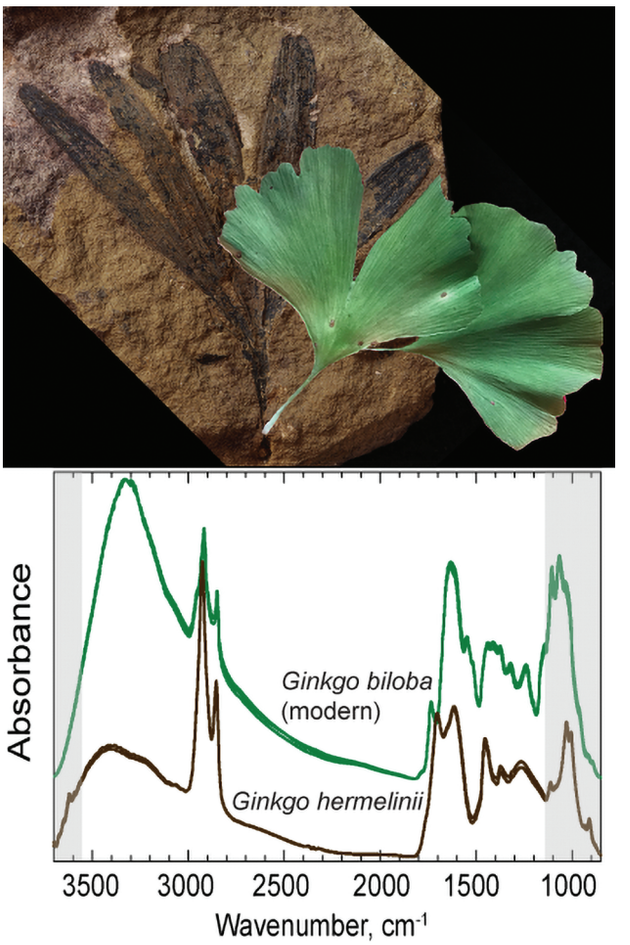

Fig. 4 Morphology and infrared absorption spectra of fossil and modern *Ginkgo* leaves. *Top*, examples of fossil *Gingko hermelinii* (S087404) from the Early Jurassic of Skåne, Dompäng, and extant *Ginkgo biloba* from an author's garden in Lund, Sweden. *Bottom*, infrared absorption spectra of *G. hermelinii* and *G. biloba* (extant) recorded at three points on each cuticle sample showing correspondence of some absorption peaks. Gray areas denote the mineral kaolinite spectral peaks in the spectra of the fossil cuticles.

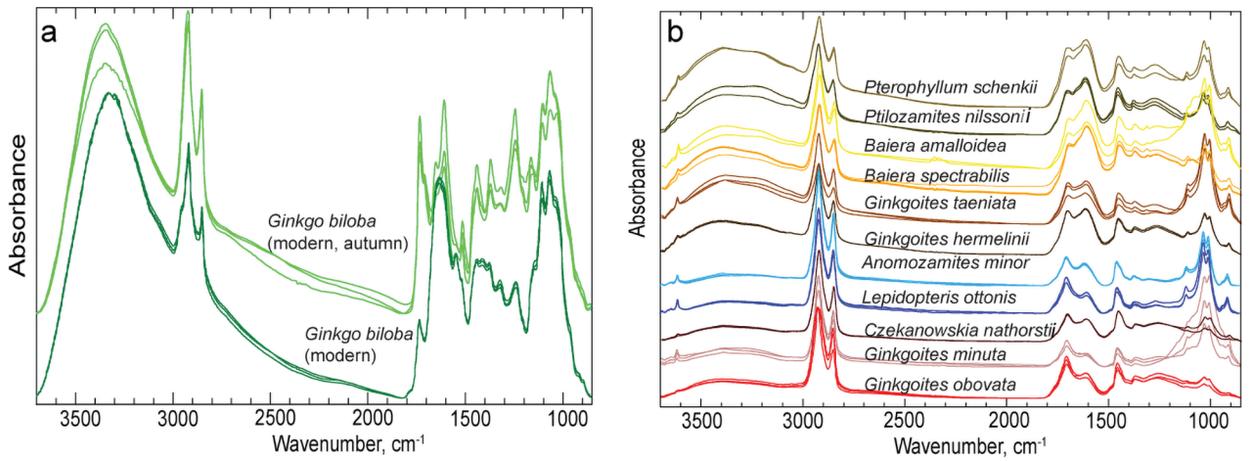

Fig. 5 Infrared absorption spectra of modern and fossil ginkgoalean cuticles. *a*, Spectra of cuticles from fresh and yellow autumn leaves of modern *Ginkgo biloba*. *b*, Spectra of fossil ginkgoalean cuticles.

predominantly to C-C vibrations in aromatic rings of phenolic compounds, but the presence of proteins is also confirmed by amide I (C=O) and amide II (N-H) bands at 1658 cm^{-1} and 1549 cm^{-1}, respectively. Bands below 1300 cm^{-1}—at 1240 and 1145 cm^{-1} (shoulder at 1164 cm^{-1}) and at 1106, 1066, and 1035 cm^{-1} (shoulder at 1016 cm^{-1})—are due to C-O-C and C-O vibrations, mostly in polysaccharides (e.g., cellulose; Mösle et al. 1998).

The most significant chemical changes caused by initial decomposition processes within cuticles of autumn leaves of modern *G. biloba*, compared with the cuticles of fresh leaves, are the disappearance of proteins (fig. 5*a*). This is indicated by a significant decrease in relative intensities of amide I (1658 cm^{-1}) and amide II (1549 cm^{-1}) bands in the corresponding IR absorption spectra (fig. 5*a*). Another interesting feature is an increase in relative intensity of an ester carbonyl–related band at 1734 cm^{-1} and appearance of an additional shoulder at 1707 cm^{-1} assigned to C=O stretching vibrations in carboxyl/ketone functional groups. This assignment is supported by the appearance of a band at 1440 cm^{-1} related to OH bending vibrations in carboxyl compounds. As will be discussed later in this article, a carboxyl/ketone-related spectral band peaking at approximately 1710 cm^{-1} is evident in the spectra of all the fossil leaves. Intensity increase of the ester carbonyl band is followed by an increase in intensity of related bands at 1245 and 1164 cm^{-1} assigned to C-OH vibrations in the group.

The spectra of the fossil leaves are dominated by spectral bands at 2926, 2855, and 1458 cm^{-1} of CH_x groups and between 1700 and 1520 cm^{-1} of aromatic compounds (figs. 4, 5*b*, 6–8). Collectively, they can be assigned to kerogen—a group of organic carbon materials formed during fossilization processes of organic compounds (Ujiié 1978; Bobroff et al. 2016). As mentioned above, the ester carbonyl band in the fresh cuticles is replaced by a band at 1702–1711 cm^{-1} (the peak position varies slightly among samples) assigned to C=O stretching vibration of carboxylic acids/ketones. Among the fossil cuticles, the most significant difference in the IR absorption spectra of the various taxa is in the absorption intensity ratio of carboxyl/ketone and aromatic carbon bands. For instance, in the spectra of *Ginkgoites obovata*, *Ginkgoites minuta*, *Czekanowskia nathorstii*, and the nonginkgoalean seed plants *Lepidopteris ottonis* and *Anomozamites minor*, this ratio is much higher than in the spectra of other taxa, meaning that *Pterophyllum*, *Ptilozamites*, and *Baeira* have the most intensive aromatic peaks (relatively, the most aromatic), while *Ginkgoites hermelinii* and *Ginkgoites taeniata* are somewhere in between.

Cluster analysis. HCA was performed to test whether it is possible to consistently distinguish the various species of Ginkgoales using the IR absorption spectra and to assess the relative similarities between the chemospectral signatures of these taxa (fig. 6*a*). The IR absorption spectra of modern *G. biloba* cuticles, including those obtained from autumn leaves, are clearly distinct from those of all fossil species, representing the significantly different chemistry of the modern leaf cuticle compared with that of all the fossil examples. This difference is considerably greater than the variation between the collective fossil taxa. This is a consequence of diagenetic changes affecting the fossil leaves compared with the unaltered extant *G. biloba*.

Two major subclusters were identified among the fossil ginkgoalean cuticles, one comprising *G. obovata* (Rhaetian, ca. 203 Ma), *G. minuta* (Rhaetian, ca. 202 Ma), and *C. nathorstii* (Hettangian, ca. 199 Ma). The second subcluster incorporates the fossil species *G. hermelinii* (Hettangian, ca. 200 Ma), *G. taeniata* (Hettangian, ca. 200 Ma), *Baiera spectabilis* (Hettangian, ca. 199 Ma), and *Baiera amalloidea* (Rhaetian, ca. 202 Ma). Both major subclusters incorporate taxa from different stratigraphic levels.

To resolve whether taxonomic affinities are reflected in the HCA dendrograms, as suggested by spectra of the *Baiera* cuticles from different stratigraphic levels clustering together, we included a selection of out-group taxa, represented by fossil cuticles of *L. ottonis*, *Pterophyllum schenkii*, *Ptilozamites nilssonii*, and *A. minor* collected from the same succession, in the HCA (fig. 6*b*) and PCA (fig. 8*c*). *Pterophyllum schenkii* and *P. nilssonii* group closely within the second branch of the dendrogram, which also includes *G. hermelinii*, *G. taeniata*, *B. spectabilis*, and *B. amalloidea*, whereas *L. ottonis* and *A. minor* cluster on the first branch with *G. obovata*, *G. minuta*, and *C. nathorstii*. Within-species groupings remain consistent; hence, factors other than taxon affinity influence the overall clustering. The specimens from both Triassic and Jurassic strata are mixed within the two branches, which suggests

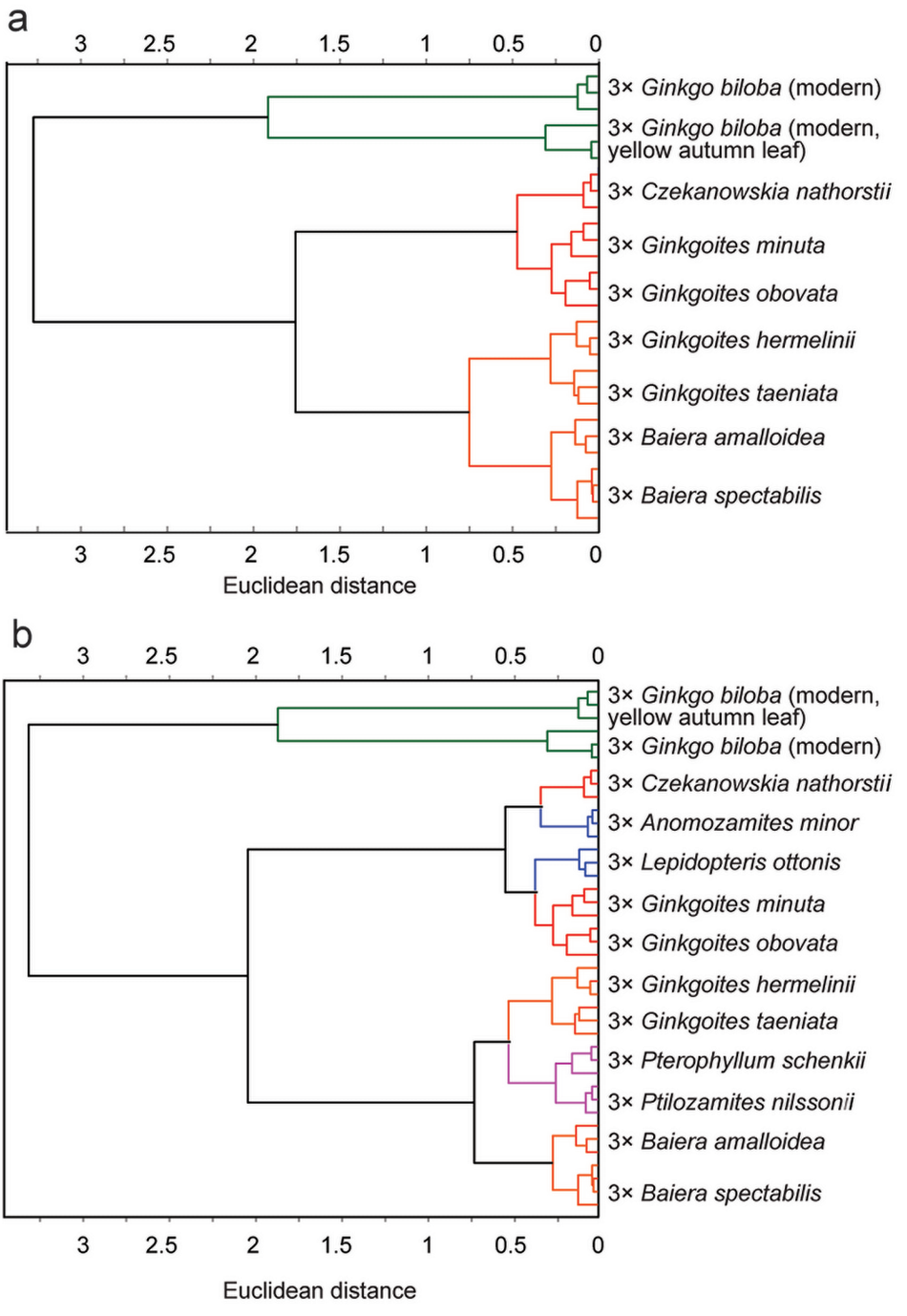

Fig. 6 Dendrograms based on hierarchical cluster analysis of infrared (IR) absorption spectra of cuticles from modern and fossil ginkgoaleans. *a*, Dendrogram including all fossil taxa and their modern counterpart *Ginkgo biloba*. *b*, Dendrogram including an out-group constituted from cuticles from fossil *Pterophyllum schenkii*, *Ptilozamites nilssonii*, *Lepidopteris ottonis*, and *Anamozamites minor*. This dendrogram also includes IR absorption spectra from yellow autumn leaves of modern *G. biloba*, which cluster on the same subcluster but with significant distance from the fresh leaves.

that diagenetic history is not the decisive factor for the clustering result.

We also plotted a heat map (fig. 7), where positive (red) and negative (blue) contributions of different first-derivative spectral bands to the HCA results are summarized. For instance, *G. minuta*, *G. obovata*, and *C. nathorstii* are clearly differentiated not only by the higher ratio of carboxyl/ketone (~1710 cm^{-1}) to aromatic (1500–1650 cm^{-1}) carbon bands but also by the relative

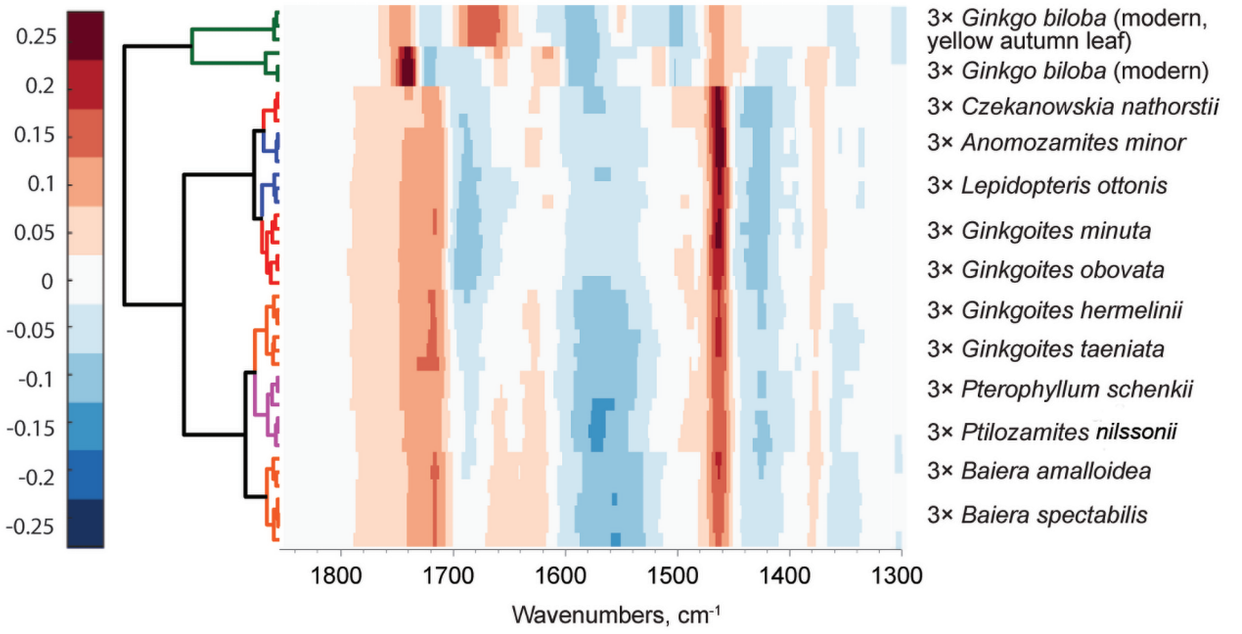

Fig. 7 Heat map showing positive (red) and negative (blue) contributions of different first-derivative spectral bands to the hierarchical cluster analysis results (dendrogram shown on the left). The intensity of the colors at certain wave numbers indicates relative abundance of corresponding functional groups, and the gradient between colors indicates the sharpness (overlapping) of the spectral features.

intensity increase at ca. 1460 and 1350 cm^{-1} representing aliphatic CH_x groups.

PCA. The three principal components shown in figure 8 and obtained through PCA collectively explain 95% of variance in the spectra. PC plots including both ginkgoaleans and the outgroup species (fig. 8*a*, 8*b*) and the respective PC loadings (fig. 8*c*) corroborate the HCA results. Within the PC1, modern *G. biloba* groups separately from all the fossil taxa, with the autumn leaves clearly distinguished. Within PC2 and PC3, the fossil taxa form the same clusters evident in the dendrograms. The clusters of fossil taxa appear to form a gradient along the PC axes; however, removing the highly separated modern species alleviates this plotting effect while not affecting the overall grouping (fig. S1). The PC loadings (figs. 8*c*, S1*c*) also confirm, as already seen in the heat map in figure 7, that carboxyl/ketone (~1710 cm^{-1}), aromatic (1500–1650 cm^{-1}), and CH_x (1470–1350 cm^{-1}) functional groups are the most important spectral features influencing the separation between the two clusters of fossil cuticles.

Discussion and Conclusion

Our IR data show that a range of stable organic compounds is present in all the analyzed material. The results further show that the breakdown of proteins and changes in other unstable organic compounds take place as soon as the leaves are shed, as evidenced by the presence of carboxyl/ketone molecules in both the extant autumn leaves and the fossil *Ginkgo* leaves but not in the fresh, green *Ginkgo* leaves.

Several factors complicate the interpretations of the fossil leaves. For example, age and phylogenetic relationship may be naturally linked—reflecting a true evolutionary signature, whereas external factors, such as pCO_2, fluctuated across the sampled interval. We can state with confidence that repeated measurements from different parts of the same leaf provided identical spectra and so did the results of analyses from different leaves of the same taxon. We can further confidently state that the biochemical signatures of fossil cuticles analyzed in this study are not functions of the diagenetic or lithological characters of the sediments hosting the fossil because different taxa from the same bed do not necessarily cluster, and different taxa from separate beds may indeed exhibit nearly identical spectra.

The major outstanding question is whether the spectral groupings are related to the environmental conditions in which the analyzed gingkoaleans grew or to true phylogenetic relationships or both. On the basis of studies of extant plant cuticles and fossil taxa with known phylogenetic relationships, we have previously shown that phylogenetic groupings at higher taxonomic levels can indeed be identified (Vajda et al. 2017). However, in this study we are comparing cuticles at the species level—taxa for which we do not know the true phylogenetic relationships.

Previous plant physiological studies have shown that external factors, such as low temperatures, UV levels, drought, light levels, and salinity, may affect leaf cuticle thickness (Poort 2009; Bacon et al. 2016). On the basis of sedimentological features combined with carbon isotope data from Astartekløft, Scoresby Sound, factors such as drought, cooling, and high salinity were excluded as factors significantly affecting the vegetation (Soh et al. 2017). To the contrary, there is evidence for intense global warming across the Triassic-Jurassic boundary, and both marine sediments and invertebrates are lacking from the successions, thus supporting a continental swamp setting with no influence of salinity (McElwain et al. 2007; Bacon et al. 2016; Soh et al. 2017).

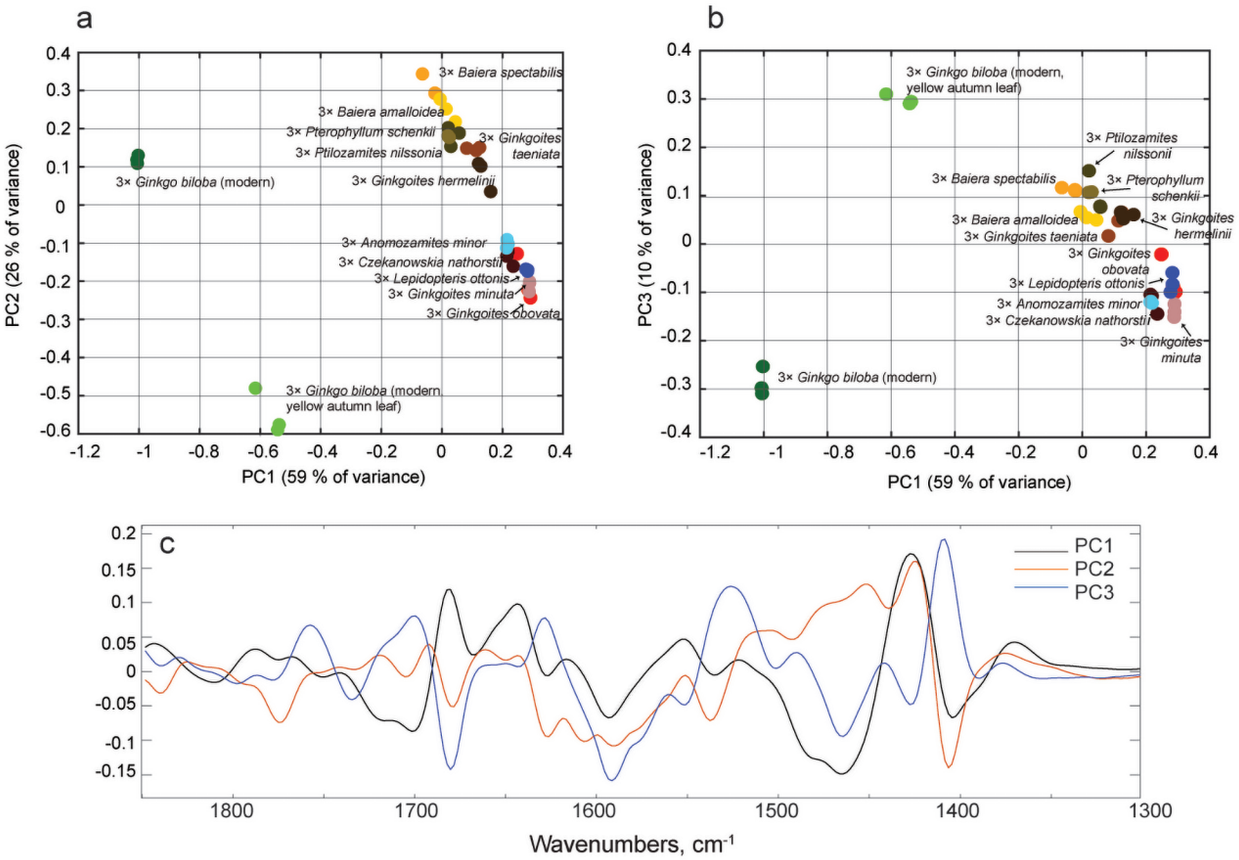

Fig. 8 *a*, *b*, Principal components (PCs) analysis score plots based on infrared absorption spectra of the cuticles of fossil and modern Ginkgoales as well as out-group taxa. *c*, PC loading plot of the first three PCs.

We interpret the groupings to reflect a combination of phylogeny and environmental factors: the environment seems to have the strongest influence when analyzing closely related species. The two oldest taxa that experienced growth during the relatively low-pCO_2 "preevent world," *Ginkgo obovata* and *Ginkgo minuta*, cluster with *Czekanowskia nathorstii*, which grew in the low-pCO_2 "postevent world" during the recovery interval (figs. 1, 6). The Early Jurassic *Ginkgo hermelinii* and *Ginkgo taeniata* cluster closely, and these taxa are both known to have similar cuticle morphology to the extent that they are difficult to distinguish morphologically (Harris 1935). They also lived in the same habitats at the same time, making it impossible to resolve the most decisive factor contributing to the differences in functional groups represented in the cuticles. The Late Triassic *Baiera amalloidea* and the Early Jurassic *Baiera spectabilis* group closely together, although they existed several million years apart but, importantly, both under high pCO_2 levels. Our results suggest that, on a biochemical basis, *Baiera* plot within the range of variation expressed by *Ginkgo*. This implies that the morphological features differentiating *Baiera* may be only of infrageneric significance within an expanded concept of *Ginkgo*. This was already suggested over 80 yr ago by Harris (1937), who questioned Florin's division of the Ginkgoales into *Ginkgo*, *Baeira*, and *Sphenobaiera* (Florin 1949). Instead, Harris showed that the venation patterns used for the division of these genera are not consistent but rather variable.

A very generalized pattern emerging for the seven ginkgoalean taxa is that the groupings may be linked to the pCO_2 levels, which in some cases seem to override the phylogeny (fig. 1). The question concerning the influence of pCO_2 on cuticle chemistry remains unresolved. A recent study by Jardine et al. (2019) addressed this issue via a meticulous experiment to test for the effects of pCO_2 variations on *Ginkgo biloba* leaf cuticle chemistry. By using attenuated total reflectance Fourier transform IR spectroscopy on leaves from plants grown in chambers with enhanced pCO_2 conditions, they showed that pCO_2 had little effect on the cuticle chemistry (Jardine et al. 2019). However, an experiment with limited short-term elevated pCO_2 in growth chambers may not accurately reflect the influence on Ginkgoales cuticle in the past, such as in the Mesozoic greenhouse world, when plants were both adapted to and grew naturally over many generations under highly elevated pCO_2. Thus, the possibility remains that pCO_2 may be an additional factor influencing the clustering of IR absorption spectra, and this should be investigated further.

The shift to higher CO_2 levels across the Triassic-Jurassic boundary has been inferred to have contributed to a global temperature rise of 3°–4°C (McElwain et al. 1999), and paleoclimatic modeling revealed that this could have resulted in summer temperatures

of 36°C at the Greenland locality (Huynh and Poulsen 2005). This warming would have directly affected the plant physiognomy and possibly contributed to the contrasting expression of organic compounds between the taxa.

Adding the spectra of the nonginkgoalean seed plants adds interesting insights but also complicates the interpretations. None of the nonginkgoalean seed plants segregates as a basal branch on the dendrogram; instead, they all nest within the Ginkgoales. Clustering that is particularly problematic to explain is that *Anomozamites* and *Pterophyllum* plot on different major branches of the dendrogram, although both are considered to be typical bennettites. *Pterophyllum* clusters with the other possible bennetitte, *Ptilozamites*, and with the Jurassic high-pCO_2 gingkoalean taxa (figs. 1, 6, 8). The peltaspermalean seed fern *Lepidopteris ottonis* plots close to the older ginkoalean taxa, reflecting their similar cuticular compositions developed in a low-pCO_2 world. One problem is that many of the seed plants present in the Greenland section are potentially closely related. More remotely related groups, such as Araucariaceae and Podocarpaceae, do not appear in this region until later in the Jurassic. Even the extant *G. biloba* is possibly closely related to these early seed plants. It has been suggested that *G. biloba* is the last survivor of a once highly diverse lineage of extinct plants, including Peltaspermales (Herrera at al. 2017), which includes *L. ottonis*. The question as to whether the biochemical fingerprints are the result of a climatic influence or retention of plesiomorphic cuticular characters or both is important and yet to be resolved. Future work assessing the influence of chemical treatment of a range of cuticles would be necessary. Combining paleobotany, organic chemistry, and phylogeny involving a broader range of ginkgoalean taxa from well-constrained paleoclimatic intervals will be necessary to conclude whether taxonomical grouping and distances between the subclusters as defined by IR absorption spectra agree with the phylogenetic affinity.

Acknowledgments

This research was financially supported by a Swedish Research Council VR grant (2019-4061) to V. Vajda, a Utrecht Network Young Researchers grant to M. Pucetaite, and a Swedish Research Council VR starting grant (NT7-2016 04905) to M. Steinthorsdottir. We thank Per Uvdal and Stephen McLoughlin for scientific discussion concerning the results and Anders Engdahl and Jimmy Heimdal at MAX IV for technical assistance and scientific discussions concerning the data. Pollyanna von Knorring produced the illustrated reconstructions of the ginkgoalean leaves. We thank the Botanical Garden of Lund University, Sweden, for giving permission to sample plant leaves; Svend Visby Funder (Centre for GeoGenetics, Natural History Museum, Copenhagen, Denmark) for giving access to T. M. Harris's fossil collections; and Arden Roy Bashforth for assisting in providing ID numbers and stratigraphical information. Finally, we thank two anonymous reviewers and guest editor Dr. Anne-Laure Decombeix for constructive feedback that improved the manuscript.

Literature Cited

Akikuni K, R Hori, V Vajda, J Grant-Mackie, M Ikehara 2010 Stratigraphy of Triassic-Jurassic boundary sequences from the Kawhia coast and Awakino gorge, Murihiku Terrane, New Zealand. Stratigraphy 7:7–24.

Ami D, P Mereghetti, SM Doglia 2013 Multivariate analysis for Fourier transform infrared spectra of complex biological systems and processes. *In* L Freitas, ed. Multivariate analysis in management, engineering and the sciences. IntechOpen, London. https://doi.org/10.5772/53850.

Anderson JM, HM Anderson 2003 Heyday of the gymnosperms: systematics and biodiversity of the Late Triassic Molteno fructifications. Strelitzia 15. National Botanic Institute, Pretoria, South Africa. 398 pp.

Bacon KL, CM Belcher, SP Hesselbo, JC McElwain 2011 The Triassic-Jurassic boundary carbon-isotope excursion expressed in taxonomically identified leaf cuticles. Palaios 26:461–469.

Bacon KL, M Haworth, E Conroy, JC McElwain 2016 Can atmospheric composition influence plant fossil preservation potential via changes in leaf mass per area? a new hypothesis based on simulated palaeoatmosphere experiments. Palaeogeogr Palaeoclimatol Palaeoecol 464:51–64.

Baker J, J Trevisan, P Bassan, R Bhargava, HJ Butler, KM Dorling, PR Fielden, et al 2014 Using Fourier transform IR spectroscopy to analyze biological materials. Nat Protoc 9:1771–1791. https://www.nature.com/articles/nprot.2014.110.

Barbacka M 2011 Biodiversity and the reconstruction of Early Jurassic flora from the Mecsek Mountains (southern Hungary). Acta Palaeobot 51:127–179.

Barbacka M, G Pacyna, A Feldman-Olszewska, J Ziaja, E Bodor 2014 Triassic–Jurassic flora of Poland; floristical support of climatic changes. Acta Geol Pol 64:281–308.

Barclay RS, JC McElwain, DL Dilcher, BB Sageman 2007 The cuticle database: developing an interactive tool for taxonomic and paleoenvironmental study of the fossil cuticle record. Pages 39–55 *in* DM Jarzen, SR Manchester, GJ Retallack, SA Jarzen, eds. Advances in angiosperm paleobotany and paleoclimatic reconstruction: contributions honoring David L. Dilcher and Jack A. Wolfe. Courier Forschungsinstitut Senckenberg 258. Schweizerbart, Stuttgart, Germany.

Barclay RS, SL Wing 2016 Improving the *Ginkgo* barometer: implications for the early Cenozoic atmosphere. Earth Planet Sci Lett 439:158–171.

Bar-Joseph Z, DK Gifford, TS Jaakkola 2001 Fast optimal leaf ordering for hierarchical clustering. Bioinformatics 17(suppl):S22–S29.

Bauer K, E Kustatscher, M Krings 2013 The ginkgophytes from the German Kupferschiefer (Permian), with considerations on the taxonomic history and use of *Baiera* and *Sphenobaiera*. Bull Geosci 88:539–556.

Beerling DJ, JC McElwain, CP Osborne 1998 Stomatal responses of the "living fossil" *Ginkgo biloba* L. to changes in atmospheric CO_2 concentrations. J Exp Bot 49:1603–1607.

Boatman EM, MB Goodwin, H-YN Holman, S Fakra, W Zheng, R Gronsky, MH Schweitzer 2019 Mechanisms of soft tissue and protein preservation in *Tyrannosaurus rex*. Sci Rep 9:15678.

Bobroff V, HH Chen, S Javerzat, C Petibois 2016 What can infrared spectroscopy do for characterizing organic remnant in fossils? Trends Anal Chem 82:443–456.

Bonis N, J Van Konijnenburg-Van Cittert, W Kürschner 2010 Changing CO_2 conditions during the end-Triassic inferred from stomatal frequency analysis on *Lepidopteris ottonis* (Goeppert) Schimper and *Ginkgoites taeniatus* (Braun) Harris. Palaeogeogr Palaeoclimatol Palaeoecol 295:146–161.

Chen LQ, CS Li 2004 The epidermal characters and stomatal development of *Ginkgo biloba*. Bull Bot Res 24:417–422.

Chen LQ, CS Li, WG Chaloner, DJ Beerling, QS Sun, ME Collinson, PL Mitchell 2001 Assessing the potential for the stomatal characters of extant and fossil *Ginkgo* leaves to signal atmospheric CO_2 change. Am J Bot 88:1309–1315.

Crane PR 2019 An evolutionary and cultural biography of ginkgo. Plants People Planet 1:32–37.

Cruz MDR, FIF Duro 1999 New data on the kaolinite-potassium acetate complex. Clay Miner 34:565–577.

D'Angelo JA, LB Escudero, W Volkheimer, EL Zodrow 2011 Chemometric analysis of functional groups in fossil remains of the *Dicroidium* flora (Cacheuta, Mendoza, Argentina): implications for kerogen formation. Int J Coal Geol 87:97–111. https://doi.org/10.1016/j.coal.2011.05.005.

D'Angelo JA, EL Zodrow 2015 Chemometric study of structural groups in medullosalean foliage (Carboniferous, fossil Lagerstätte, Canada): chemotaxonomic implications. Int J Coal Geol 138:42–54. https://doi.org/10.1016/j.coal.2014.12.003.

——— 2018 Density and biomechanical properties of fossil fronds: a case study of *Neuropteris ovata* (seed fern, Late Pennsylvanian, Canada). Int J Coal Geol 198:63–76. https://doi.org/10.1016/j.coal.2018.09.003.

——— 2020 Preservation of *Neuropteris ovata* in roof shale and in fluvial crevasse-splay facies (Late Pennsylvanian, Sydney coalfield, Canada). I. An infrared-based chemometric model. Palaios 35:94–109. https://doi.org/10.2110/palo.2019.074.

D'Angelo JA, EL Zodrow, A Camargo 2010 Chemometric study of functional groups in Pennsylvanian gymnosperm plant organs (Sydney Coalfield, Canada): implications for hemotaxonomy and assessment of kerogen formation. Org Geochem 41:1312–1325.

Domenighini A, M Giordano 2009 Fourier transform infrared spectroscopy of microalgae as a novel tool for biodiversity studies, species identification, and the assessment of water quality. J Phycol 45:522–531.

Dupont-Nivet G, PE Jardine, C Hoorn, MAM Beer, N Barbolini, A Woutersen, G Bogotá-Angel, et al 2021 Sporopollenin chemistry and its durability in the geological record: an integration of extant and fossil chemical data across the seed plants. Palaeontology 64:285–305.

Fan XX, L Shen, X Zhang, XY Chen, CX Fu 2004 Assessing genetic diversity of *Ginkgo biloba* L. (Ginkgoaceae) populations from China by RAPD markers. Biochem Genet 42:269–278.

Florin R 1949 The morphology of *Trichopitys heteromorpha*, a seed plant of Paleozoic age, and the evolution of the female flowers in the Ginkgoinea. Acta Horti Bergiani 15:79–109.

Fraser WT, AC Scott, AES Forbes, IJ Glasspool, RE Plotnick, F Kenig, BH Lomax 2012 Evolutionary stasis of sporopollenin biochemistry revealed by unaltered Pennsylvanian spores. New Phytol 196:397–401.

Fraser WT, MA Sephton, JS Watson, S Self, BH Lomax, DI James, CH Wellman, TV Callaghan, DJ Beerling 2011 UV-B absorbing pigments in spores: biochemical responses to shade in a high-latitude birch forest and implications for sporopollenin-based proxies of past environmental change. Polar Res 30:8312.

Gautam R, S Vanga, F Ariese, S Umapathy 2015 Review of multidimensional data processing approaches for Raman and infrared spectroscopy. EPJ Tech Instrum 2:1–38. https://doi.org/10.1140/epjti/s40485-015-0018-6.

Ge Y-Q, Y-X Qiu, B-Y Ding, C-X Fu 2003 An ISSR analysis on population genetic diversity of the relict plant *Ginkgo biloba*. Biodivers Sci 11:276–287.

Gong W, C Chen, C Dobes, CX Fu, MA Koch 2008 Phylogeography of a living fossil: Pleistocene glaciations forced *Ginkgo biloba* L. (Ginkgoaceae) into two refuge areas in China with limited subsequent postglacial expansion. Mol Phylogenet Evol 48:1095–1105.

Gordenko NV, AV Broushkin 2015 Ginkgoales: some problems of systematics and phylogeny. Paleontol J 5:94–100.

Guignard G 2019 Thirty-three years (1986–2019) of fossil plant cuticle studies using transmission electron microscopy: a review. Rev Palaeobot Palynol 271:104097. https://doi.org/10.1016/j.revpalbo.2019.07.002.

Harris TM 1926 The Rhaetic flora of Scoresby Sound, East Greenland. Bianco Lunos, Copenhagen. 147 pp.

——— 1931 The fossil flora of Scoresby Sound, East Greenland. 1. Cryptogams. Medd Grønl 85:1–140.

——— 1932*a* The fossil flora of Scoresby Sound, East Greenland. 2. Seed plants incertae sedis. Medd Grønl 85:1–141.

——— 1932*b* The fossil flora of Scoresby Sound, East Greenland. 3. Caytoniales and Bennettitales. Medd Grønl 85:1–133.

——— 1935 The fossil flora of Scoresby Sound, East Greenland. 4. Ginkgoales, Lycopodiales and isolated fructifications. Medd Grønl 112:1–121.

——— 1937 The fossil flora of Scoresby Sound, East Greenland. 5. Stratigraphic relations of the plant beds. Medd Grønl 112:1–123.

Herrera F, G Shi, N Ichinnorov, M Takahashi, EV Bugdaeva, PS Herendeen, PR Crane 2017 The presumed ginkgophyte *Umaltolepis* has seed-bearing structures resembling those of Peltaspermales and Umkomasiales. Proceedings of the National Academy of Sciences of the USA 114:E2385–E2391.

Hesselbo SP, SA Robinson, F Surlyk, S Piasecki 2002 Terrestrial and marine extinction at the Triassic-Jurassic boundary synchronized with major carbon-cycle perturbation: a link to initiation of massive volcanism? Geology 30:251–254.

Huynh TT, CJ Poulsen 2005 Rising atmospheric CO_2 as a possible trigger for the end-Triassic mass extinction. Palaeogeogr Palaeoclimatol Palaeoecol 217:223–242.

Jansson I-M, S McLoughlin, V Vajda, M Pole 2008 An Early Jurassic flora from the Clarence-Moreton Basin, Australia. Rev Palaeobot Palynol 150:5–21.

Jardine PE, FAJ Abernethy, BH Lomax, WD Gosling, WT Fraser 2017 Shedding light on sporopollenin chemistry, with reference to UV reconstructions. Rev Palaeobot Palynol 238:1–6.

Jardine PE, WT Fraser, WD Gosling, CN Roberts, WJ Eastwood, BH Lomax 2020 Proxy reconstruction of ultraviolet-B irradiance at the Earth's surface, and its relationship with solar activity and ozone thickness. Holocene 30:155–161.

Jardine PE, WT Fraser, BH Lomax, MA Sephton, TM Shanahan, CS Miller, WD Gosling 2016 Pollen and spores as biological recorders of past ultraviolet irradiance. Sci Rep 6:1–8.

Jardine PE, M Kent, WT Fraser, BH Lomax 2019 *Ginkgo* leaf cuticle chemistry across changing pCO_2 regimes. PalZ 93:549–558.

Kovács EB, M Ruhl, A Demény, I Fórizs, I Hegyi, ZR Horváth-Kostka, F Móricz, Z Vallner, J Pálfy 2020 Mercury anomalies and carbon isotope excursions in the western Tethyan Csövár section support the link between CAMP volcanism and the end-Triassic extinction. Glob Planet Change 194:103291.

Kustatscher E, SR Ash, E Karasev, C Pott, V Vajda, J Yu, S McLoughlin 2018 Flora of the Late Triassic. Pages 545–622 *in* LH Tanner, ed. Late Triassic of the world: Earth in a time of transition. Topics in Geobiology 46. Springer, Cham, Switzerland.

Lindgren J, P Sjövall, RM Carney, P Uvdal, J Gren, G Dyke, B Pagh Schultz, MD Shawkey, KR Barnes, MJ Polcyn 2014 Skin pigmentation provides evidence of convergent melanism in extinct marine reptiles. Nature 506:484–488.

Lindgren J, P Sjövall, V Thiel, W Zheng, S Ito, K Wakamatsu, R Hauff, et al 2018 Soft-tissue evidence for homeothermy and crypsis in a Jurassic ichthyosaur. Nature 564:359–365.

Lindström S, B van de Schootbrugge, KH Hansen, GK Pedersen, P Alsen, N Thibault, K Dybkjær, CJ Bjerrum, LH Nielsen 2017 A new correlation of Triassic-Jurassic boundary successions in NW Europe, Nevada and Peru, and the Central Atlantic Magmatic Province: a time-line for the end-Triassic mass extinction. Palaeogeogr Palaeoclimatol Palaeoecol 478:80–102.

Liu N, C Karunakaran, R Lahlali, T Warkentin, RA Bueckert 2019 Genotypic and heat stress effects on leaf cuticles of field pea using ATR-FTIR spectroscopy. Planta 249:601–613.

Lomax BH, WT Fraser, G Harrington, S Blackmore, MA Sephton, NBW Harris 2012 A novel palaeoaltimetry proxy based on spore and pollen wall chemistry. Earth Planet Sci Lett 353–354:22–28.

Lundblad AB 1949 De geologiska resultaten från borrningarna vid Höllviken. 4. On the presence of *Lepidopteris* in cores from "Höllviken II." Sver Geol Unders Ser C 507:1–11.

——— 1959*a* Rhaeto-Liassic floras and their bearing on the stratigraphy of Triassic–Jurassic rocks. Stockh Contr Geol 3:83–102.

——— 1959*b* Studies in the Rhaeto-Liassic floras of Sweden. II. Ginkgophyta from the mining district of NW Scania. K Vet Akad Handl Fjärde Ser 6:1–38.

Mander L, WM Kürschner, J McElwain 2013 Palynostratigraphy and vegetation history of the Triassic–Jurassic transition in East Greenland. J Geol Soc 170:37–46.

Mark H, J Workman 2003 Derivatives in spectroscopy. II. The true derivative. Spectroscopy 18:25–28.

Marzoli AS, S Callegaro, J Dal Corso, JH Davies, M Chiaradia, N Youbi, H Bertrand, L Reisberg, R Merle, F Jourdan 2018 The Central Atlantic magmatic province (CAMP): a review. Pages 91–125 *in* LH Tanner, ed. The Late Triassic world. Springer, Syracuse, NY.

Mays C, M Steinthorsdottir, JD Stilwell 2015 Climatic implications of *Ginkgoites waarrensis* Douglas emend. from the south polar Tupuangi flora, Late Cretaceous (Cenomanian), Chatham Islands. Palaeogeogr Palaeoclimatol Palaeoecol 438:308–326.

McElwain JC, D Beerling, F Woodward 1999 Fossil plants and global warming at the Triassic–Jurassic boundary. Science 285:1386–1390.

McElwain JC, ME Popa, SP Hesselbo, M Haworth, F Surlyk 2007 Macroecological responses of terrestrial vegetation to climatic and atmospheric change across the Triassic/Jurassic boundary in East Greenland. Paleobiology 33:547–573.

McElwain JC, PJ Wagner, SP Hesselbo 2009 Fossil plant relative abundances indicate sudden loss of Late Triassic biodiversity in East Greenland. Science 324:1554–1556.

McLoughlin S 2017 Antarctic *Glossopteris* forests. Pages 22–23 *in* A Cullum, AW Martinius, eds. 52 more things you should know about palaeontology. Agile Libre, Nova Scotia.

——— 2021 History of life: plants: gymnosperms. Pages 476–500 *in* S Elias, D Alderton, eds. Encyclopedia of geology. 2nd ed. Elsevier, Amsterdam.

Meller B, R Zetter, A Hassler, JM Bouchal, C-C Hofmann, Friðgeir Grímsson 2015 Middle Miocene macrofloral elements from the Lavanttal Basin, Austria. I. *Ginkgo adiantoides* (Unger) Heer. Austrian J Earth Sci 108:185–198.

Meyen SV 1984 Basic features of gymnosperm systematics and phylogeny as evidenced by the fossil record. Bot Rev 50:1–111.

Mösle BE, ME Collinson, P Fink, BA Stankiewicz, AC Scott, R Wilson 1998 Factors influencing the preservation of plant cuticles: a comparison of morphology and chemical composition of modern and fossil examples. Org Geochem 29:1369–1380.

Mustoe GE 2002 Eocene *Ginkgo* leaves from the Pacific Northwest. Can J Bot 80:1078–1087.

Olsen PE 1999 Giant lava flows, mass extinctions, and mantle plumes. Science 284:604–605.

Pálfy J, AT Kocsis 2014 Volcanism of the Central Atlantic Magmatic Province as the trigger of environmental and biotic changes around the Triassic-Jurassic boundary. Pages 245–261 *in* G Keller, AC Kerr, eds. Volcanism, impacts and mass extinctions: causes and effects. Geological Society of America, Boulder, CO.

Poorter H, U Niinemets, L Poorter, IJ Wright, R Villar 2009 Causes and consequences of variation in leaf mass per area (LMA): a meta-analysis. New Phytol 182:565–588.

Pott C, S McLoughlin 2011 The Rhaeto-Liassic flora from Rögla, northern Scania, Sweden. Palaeontology 54:1025–1051.

Qu Y, A Engdahl, S Zhu, V Vajda, N McLoughlin 2015 Ultrastructural heterogeneity of carbonaceous material in ancient cherts: investigating biosignature origin and preservation. Astrobiology 15:825–842.

Qu Y, N McLoughlin, MA van Zuilen, M Whitehouse, A Engdahl, V Vajda 2019 Evidence for molecular structural variations in the cytoarchitectures of a Jurassic plant. Geology 47:325–329.

Quan C, C Sun, Y Sun, G Sun 2009 High resolution estimates of paleo-CO_2 levels through the Campanian (Late Cretaceous) based on *Ginkgo* cuticles. Cretac Res 30:424–428.

Retallack GJ 2001 A 300-million-year record of atmospheric carbon dioxide from fossil plant cuticles. Nature 411:287–289.

Retallack GJ, GD Conde 2020 Deep time perspective on rising atmospheric CO_2. Glob Planet Change 189:103177.

Richard B, J McElwain, D Dilcher, BB Sageman 2007 The cuticle database: developing an interactive tool for taxonomic and paleoenvironmental study of the fossil cuticle record. Pages 39–55 *in* DM Jarzen, SR Manchester, GJ Retallack, SA Jarzen, eds. Advances in angiosperm paleobotany and paleoclimatic reconstruction: contributions honouring David L. Dilcher and Jack A. Wolfe. Courier Forschungsinstitut Senckenberg 258. Schweizerbart, Stuttgart, Germany.

Royer DL, LJ Hickey, SL Wing 2003 Ecological conservatism in the "living fossil" *Ginkgo*. Paleobiology 29:84–104.

Schobben M, J Gravendyck, F Mangels, U Struck, R Bussert, WM Kürschner, D Korn, PM Sander, M Aberhan 2019 A comparative study of total organic carbon-$\delta^{13}C$ signatures in the Triassic–Jurassic transitional beds of the Central European Basin and western Tethys shelf seas. Newsl Stratigr 52:461–486.

Sepkoski JJ 1996 Patterns of Phanerozoic extinction: a perspective from global data bases. Pages 35–51 *in* OH Walliser, ed. Global events and event stratigraphy in the Phanerozoic. Springer, Berlin.

Seyfullah LJ, E-M Sadowski, A Schmidt 2015 Species-level determination of closely related araucarian resins using FTIR spectroscopy and its implications for the provenance of New Zealand amber. PeerJ 3:e1067.

Shen L, X-Y Chen, X Zhang, Y-Y Li, C-X Fu, Y-X Qiu 2005 Genetic variation of *Ginkgo biloba* L. (Ginkgoaceae) based on cpDNA PCR-RFLPs: inference of glacial refugia. Heredity 94:396–401.

Slodownik M, V Vajda, M Steinthorsdottir 2021 Fossil seed fern *Lepidopteris ottonis* from Sweden records increasing CO_2 concentration during the end-Triassic extinction event. Palaeogeogr Palaeoclimatol Palaeoecol 564:11057.

Smith JV, Y Luo 2004 Studies on molecular mechanisms of *Ginkgo biloba* extract. Appl Microbiol Biotechnol 64:465–472.

Smith RY, DR Greenwood, JF Basinger 2010 Estimating paleoatmospheric pCO_2 during the Early Eocene Climatic Optimum from stomatal frequency of *Ginkgo*, Okanagan Highlands, British Columbia, Canada. Palaeogeogr Palaeoclimatol Palaeoecol 293:120–131.

Soh WK, IJ Wright, KL Bacon, TI Lenz, M Steinthorsdottir, AC Parnell, JC McElwain 2017 Palaeo leaf economics reveal a shift in ecosystem function associated with the end-Triassic mass extinction event. Nat Plants 3:17104.

Steemans P, K Lepot, CP Marshall, A Le Hérissé, EJ Javaux 2010 FTIR characterisation of the chemical composition of Silurian miospores (cryptospores and trilete spores) from Gotland, Sweden. Rev Palaeobot Palynol 162:577–590.

Steinthorsdottir M, KL Bacon, ME Popa, L Bochner, JC McElwain 2011*a* Bennettitalean leaf cuticle fragments (here *Anomozamites* and *Pterophyllum*) can be used interchangeably in stomatal frequency-based palaeo-CO_2 reconstructions. Palaeontology 54:867–882.

Steinthorsdottir M, AJ Jeram, JC McElwain 2011*b* Extremely elevated CO_2 concentrations at the Triassic/Jurassic boundary. Palaeogeogr Palaeoclimatol Palaeoecol 308:418–432.

Steinthorsdottir M, V Vajda 2015 Early Jurassic (Pliensbachian) CO_2 concentrations based on stomatal analysis of fossil conifer leaves from eastern Australia. Gondwana Res 27:932–939.

Steinthorsdottir M, FI Woodward, F Surlyk, JC McElwain 2012 Deep-time evidence of a link between elevated CO_2 concentrations and perturbations in the hydrological cycle via drop in plant transpiration. Geology 40:815–818.

Sun B, L Xiao, S Xie, S Deng, Y Wang, H Jia, S Turner 2007 Quantitative analysis of paleoatmospheric CO_2 level based on stomatal characters of fossil *Ginkgo* from Jurassic to Cretaceous of China. Acta Geol Sin 81:931–939.

Sun C-L, X Tan, DL Dilcher, H Wang, Y-L Na, T Li, Y-F Ly 2018 Middle Jurassic *Ginkgo* leaves from the Daohugou area, Inner Mongolia, China and their implication for palaeo-CO_2 reconstruction. Palaeoworld 27:46–481.

Sun Y, X Li, G Zhao, H Liu, Y Zhang 2016 Aptian and Albian atmospheric CO_2 changes during oceanic anoxic events: evidence from fossil *Ginkgo* cuticles in Jilin Province, Northeast China. Cretac Res 62:130–141.

Taylor TN, EL Taylor 1993 The biology and evolution of fossil plants. Prentice Hall, Englewood Cliffs, NJ. 982 pp.

Taylor TN, EL Taylor, M Krings 2006 Mesozoic seed ferns: old paradigms, new discoveries. J Torrey Bot Soc 133:62–82.

——— 2009 Paleobotany: the biology and evolution of fossil plants. Elsevier, London. 1230 pp.

Tralau H 1968 Evolutionary trends in the genus *Ginkgo*. Lethaia 1:63–101.

Ujiié Y 1978 Kerogen maturation and petroleum genesis. Nature 272:438–439.

Vajda V, M Calner, A Ahlberg 2013 Palynostratigraphy of dinosaur footprint-bearing deposits from the Triassic-Jurassic boundary interval of Sweden. GFF 135:120–130.

Vajda V, M Pucetaite, S McLoughlin, A Engdahl, J Heimdal, P Uvdal 2017 Molecular signatures of fossil leaves provide unexpected new evidence for extinct plant relationships. Nat Ecol Evol 1:1093–1099.

Vajda V, J Wigforss-Lange 2009 Onshore Jurassic of Scandinavia and related areas. GFF 131:5–23.

van Bergen PF, ME Collinson, DEG Briggs, JW De Leeuw, AC Scott, RP Evershed, P Finch 1978 Resistant biomacromolecules in the fossil record. Acta Bot Neerl 44:319–342.

Woodward FI 1987 Stomatal numbers are sensitive to increases in CO_2 from preindustrial levels. Nature 327:617–618.

Wu J, S Ding, Q Li, B Sun, Y Wang 2016 Reconstructing paleoatmospheric CO_2 levels based on fossil Ginkgoites from the Upper Triassic and Middle Jurassic in Northwest China. PalZ 90:377–387.

Yapp CJ, H Poths 1996 Carbon isotopes in continental weathering environments and variations in ancient atmospheric CO_2 pressure. Earth Planet Sci Lett 137:71–82.

Zhang L, T Yang, W-J Li, J-W Jia, X-S Mou, Y-Q Chen, S-P Xie, J-J Fan, D-F Yan 2019 Reading paleoenvironmental information from Middle Jurassic ginkgoalean fossils in the Yaojie and Baojishan basins, Gansu Province, China. Geobios 52:99–106.

Zhou M, T Hua, X Ma, H Sun, L Xu 2019 Protein content and amino acids profile in 10 cultivars of ginkgo (*Ginkgo biloba* L.) nut from China. R Soc Open Sci 6:181571.

Zhou N, Y Wang, L Ya, AS Porter, WM Kurschner, L Li, N Lu, JC McElwain 2020 An inter-comparison study of three stomatal-proxy methods for CO_2 reconstruction applied to early Jurassic Ginkgoales plants. Palaeogeogr Palaeoclimatol Palaeoecol 542:109547.

Zhou Z 2009 An overview of fossil Ginkgoales. Palaeoworld 18:1–22.

Zhou Z, X Wu 2006 The rise of ginkoalean plants in the early Mesozoic: a data analysis. Geol J 41:363–375.

Zodrow EL, JA D'Angelo 2019 Chemometric-based, 3D chemical-architectural model of *Odontopteris cantabrica* Wagner (Medullosales, Pennsylvanian, Canada): implications for natural classification and taxonomy. Int J Coal Geol 207:12–25.